

Effective Linewidth due to Porosity and Anisotropy in Polycrystalline Yttrium Iron Garnet and Ca-V-Substituted Yttrium Iron Garnet at 10 GHz

CARL E. PATTON

Raytheon Research Division, Waltham, Massachusetts 02154

(Received 13 September 1968)

The field dependence of the uniform-precession relaxation rate or an effective linewidth ΔH_{eff} can provide detailed information concerning the relaxation in polycrystals. Determinations of ΔH_{eff} versus static field H_0 have been made as a function of porosity in polycrystalline yttrium iron garnet (YIG) and as a function of anisotropy in polycrystalline calcium-vanadium-substituted YIG (YCVF). The experimental results were obtained from microwave susceptibility data taken on spherical samples at room temperature and 10 GHz. Porosity in the YIG ranged from 21 to <1%. The YCVF materials had anisotropy fields from 114 to 350 Oe. Far from resonance, ΔH_{eff} is small, on the order of a few Oe, and field-independent. Near resonance, ΔH_{eff} increases sharply and exhibits a peak. The size and symmetry of the peak are functions of porosity and anisotropy. In general, ΔH_{eff} peaks at fields above the field H_{res} for resonance in the porous materials. The magnitude of the peak increases and the curve broadens considerably with increasing porosity. For the YCVF materials, ΔH_{eff} peaks below H_{res} for the low-anisotropy samples, and above for the high-anisotropy samples. The effective linewidth increases and the curves broaden with increasing anisotropy. The experimental results can be explained on the basis of two-magnon scattering from inhomogeneities related to porosity and the anisotropy in randomly oriented crystallites. The increase in ΔH_{eff} near resonance is due to coupling of the uniform-precession mode at the driving frequency to degenerate long-wavelength spin waves. Far from resonance, degenerate long-wavelength modes no longer exist, so that ΔH_{eff} is small and field-independent. The differences in the symmetry of the ΔH_{eff} peak for the different materials can be explained by differences in the coupling to the degenerate modes. The broadening of the peaks with increasing porosity and anisotropy arises from secondary scattering interactions which do not involve the uniform precession. Theoretical curves obtained from calculations which include secondary scattering are in good agreement with the data.

I. INTRODUCTION

THE relatively large linewidths observed in polycrystalline ferrimagnetic insulators are caused by inhomogeneities such as pores or the crystalline anisotropy in randomly oriented crystallites.¹ Linewidth data have been explained by examining the uniform-precession relaxation rate due to coupling with degenerate spin-wave modes at resonance. This coupling is usually termed two-magnon scattering. Among other things, the two-magnon relaxation rate depends on the density of long-wavelength spin-wave states degenerate with the uniform precession. By modifying this density of states, the relaxation rate can be changed and detailed information concerning two-magnon scattering can be obtained. One way to obtain such information is to drive the uniform precession off resonance and determine the relaxation rate from susceptibility data. The density of degenerate states can be varied over wide ranges simply by changing the static magnetic field. The results are limited only by the accuracy with which the susceptibility can be measured. A more limited technique used by several workers is to operate at resonance and measure linewidths at different frequencies,² for different sample orientations,³ or for different magnetostatic modes.^{4,5} The variation in the density of states using such an approach is usually

smaller and is harder to obtain experimentally than with the first technique.

The off-resonance susceptibility technique, first suggested by Motizuki *et al.*,⁶ has been used by Liu⁷ and by Kohane and Schlömann⁸ to determine the relaxation rate η from measurements of the imaginary part χ'' of the microwave susceptibility. This procedure is valid far from resonance. Near resonance, however, it is necessary to measure the real part χ' as well, in order to determine η .⁶ By measuring both χ' and χ'' , Vrehan⁹ has examined η near resonance for porous Ni-Zn ferrite.

The purpose of the present investigation was twofold: (a) to investigate the field dependence of the uniform-precession relaxation rate near ferromagnetic resonance for a range of garnet materials in which a large porosity or anisotropy scattering contribution to the relaxation is expected, and (b) to explain the data, insofar as possible, in terms of theoretical results concerning two-magnon scattering in insulating ferromagnets. The study provides several new conclusions concerning two-magnon scattering due to porosity and anisotropy in polycrystals: (a) The symmetry of the relaxation-rate field dependence is a strong function of both the type of scattering involved (porosity or anisotropy) and the magnitude of the scattering contribution; and (b) the data are in qualitative agreement with theoretical expectations for porosity broadening and in excellent

¹ See M. Sparks, *Ferromagnetic-Relaxation Theory* (McGraw-Hill Book Co., New York, 1964).

² C. R. Buffer, *J. Appl. Phys.* **30**, 172S (1959); **31**, 222S (1960).

³ A. Risley and H. Bussey, *J. Appl. Phys.* **35**, 896 (1964).

⁴ R. L. White, *J. Appl. Phys.* **30**, 182S (1959).

⁵ J. Nemanich, *Phys. Rev.* **136**, A1657 (1964).

⁶ K. Motizuki, M. Sparks, and P. E. Seiden, *Phys. Rev.* **140**, A972 (1965).

⁷ S. Liu, Stanford University Microwave Laboratory Report No. SUML-1092, 1963, p. 151 (unpublished).

⁸ T. Kohane and E. Schlömann, *J. Appl. Phys.* **39**, 720 (1968).

⁹ Q. H. F. Vrehan, *IEEE Trans. Magnetics* **MAG-4**, 479 (1968).

quantitative agreement with theory for anisotropy broadening. In Secs. II and III, the details of the experimental procedures will be outlined and the data presented. After a review of relevant theoretical considerations in Sec. IV, the data will be interpreted in terms of the theory in Sec. V, and the results of the investigation will be summarized in Sec. VI.

II. EXPERIMENT

The measurements were performed on spherical samples of yttrium iron garnet (YIG) and Ca-V-substituted YIG (YCVF) prepared using standard ceramic techniques.¹⁰ In the YIG materials, the porosity was controlled by a variation in sintering times. The porosity was inferred from density measurements on large blocks of the fired materials and checked with density determinations on the individual spherical samples. Materials with density ranging from more than 99 to 79% of the theoretical YIG density were obtained. The basic material was single-phase polycrystalline YIG with good microwave properties, as indicated by a ferromagnetic resonance linewidth of 25 Oe for the dense material. In the discussion to follow, the label YIG99 will denote 99% dense samples, YIG79 the 79% dense samples, etc. In Table I these materials are listed along with values of porosity and average saturation induction. The porosities given in the table represent an average of the values for the individual spherical samples. The average saturation induction was determined using a vibrating sample magnetometer.

YCVF¹¹ was used to study the effective linewidth as a function of anisotropy field. Similar Ca-V-substituted materials have been reported on previously by Van Hook *et al.*¹² By varying the amounts of substituted material according to $Y_{3-2x}Ca_{2x}Fe_{5-x}V_xO_{12}$, the average saturation induction $4\pi M$ can be varied from 1750 G for $x=0$, corresponding to YIG, to zero for $x=1$, corresponding to $YCa_2Fe_4VO_{12}$. The anisotropy constant K_1 is not a strong function of x . As a consequence the anisotropy field $H_A = 2|K_1|/M$ increases with increased vanadium content for $0 < x < 1$. In this study samples with x between 0.32 and 0.85 were used. These materials were all better than 99% dense and were single-phase. The relevant properties of these materials are summarized

TABLE I. Density (in %) of theoretical density and average saturation induction for the porous YIG materials.

| Label | Density (theoretical YIG density, 100%) (%) | Average saturation induction $4\pi M$ (G) |
|-------|---|---|
| YIG99 | >99 | 1750 |
| YIG97 | 97 | 1720 |
| YIG91 | 91 | 1640 |
| YIG84 | 84 | 1500 |
| YIG79 | 79 | 1380 |

in Table II. Anisotropy values are estimates obtained from microwave measurements on single-crystal materials.¹³ The anisotropy field varies from 114 to 350 Oe. In all of the discussion to follow, materials with $x=0.32$ will be indicated by YCVF32, $x=0.63$ by YCVF63, etc.

The data were obtained for annealed spherical samples. Unannealed samples generally exhibited much larger losses, which are presumably associated with surface damage. Relatively large 2-mm-diam spheres were used to obtain data at fields far from ferromagnetic resonance, where the susceptibility is quite small. Near resonance, $\frac{1}{2}$ -mm-diam samples were used because the large spheres caused a substantial loading of the microwave cavity. In intermediate field regions 1-mm-diam samples were used to serve as a check on the other data. The different samples were all cut from the same fired ceramic piece of each material.

The relaxation rate is related to the diagonal component of the effective susceptibility tensor χ_e defined by

$$\mathbf{m} = \chi_e \mathbf{h}, \quad (1)$$

where \mathbf{m} is the magnetization response due to an applied external microwave field \mathbf{h} , both normal to the static field direction. The diagonal component χ_e is related to the changes in cavity Q and resonant frequency of a microwave cavity due to the magnetic sample. The change in Q and the frequency shift $\delta\omega$, relative to the values at high field (8 kOe), were obtained as a function of static field utilizing a transmission cavity spectrometer at 9.96 GHz and a rectangular cavity. Most of the data were obtained with a TE_{104} cavity, although TE_{10n} configurations with $n=2$,

TABLE II. Vanadium content x , average saturation induction $4\pi M$, anisotropy constant K_1 , and anisotropy field H_A for the Ca-V-substituted garnet materials.

| Label | Vanadium content x $Y_{3-2x}Ca_{2x}Fe_{5-x}V_xO_{12}$ | Average saturation induction $4\pi M$ (G) | Anisotropy constant K_1 (erg/cm ³) | Anisotropy field $H_A = 2 K_1 /M$ (Oe) |
|--------|---|---|--|--|
| YCVF32 | 0.32 | 1220 | -5.5×10^8 | 114 |
| YCVF63 | 0.63 | 650 | -4.6×10^8 | 178 |
| YCVF70 | 0.70 | 551 | -4.4×10^8 | 200 |
| YCVF80 | 0.80 | 356 | -4.2×10^8 | 290 |
| YCVF85 | 0.85 | 265 | -3.7×10^8 | 350 |

¹⁰ See, for example, R. F. Soohoo, *Theory and Application of Ferrites* (Prentice-Hall, Inc., Englewood Cliffs, N. J., 1960).

¹¹ S. Geller, G. P. Espinosa, H. J. Williams, R. C. Sherwood, and E. A. Nesbitt, *J. Appl. Phys.* **35**, 570 (1964).

¹² H. J. Van Hook, J. J. Green, F. Euler, and E. R. Czerlinsky, *J. Appl. Phys.* **39**, 730 (1968).

¹³ F. Euler and H. J. Van Hook (private communication).

6, or 8 were used in some cases for increased sensitivity or reduced loading for particular samples. The spectrometer was similar to that described previously by Green and Kohane.¹⁴ Frequency measurements were made by a heterodyning technique utilizing a stabilized reference frequency source. Frequency, relative to the reference, could be determined to ± 1 kHz. Standard cavity perturbation theory (see Ref. 14) was used to determine the real part χ_e' and the negative imaginary part χ_e'' of χ_e as a function of static field.

Values of χ_e' and χ_e'' were used to calculate the relaxation rate η and the associated effective linewidth ΔH_{eff} as a function of static field. By assuming a phenomenological equation of motion for the magnetization which includes relaxation,¹⁵ χ_e can be calculated explicitly and is given by

$$\chi_e = (\chi_e' - i\chi_e'') = \frac{\gamma M (\gamma H_0 + i\eta)}{(\gamma H_0 + i\eta)^2 - \omega^2}, \quad (2)$$

for spherical samples, where H_0 is the static external magnetic field, ω is the excitation frequency, and γ is the gyromagnetic ratio. With χ_e' and χ_e'' determined experimentally, the real and imaginary parts of Eq. (2) constitute two equations in two unknowns, η and γ . The gyromagnetic ratio γ is usually quite close to the free-electron value of $1.76 \times 10^7 \text{ Oe}^{-1} \text{ sec}^{-1}$. An approximate solution for η and γ can be easily obtained if γM in the numerator of Eq. (2) is replaced by $\gamma_0 M$, where γ_0 is the free-electron gyromagnetic ratio. With this replacement, Eq. (2) is simply a complex quadratic equation in $\Omega_0 = \gamma H_0 + i\eta$ which can be solved explicitly for γ and η . A more exact solution can be obtained by an iterative procedure in which the calculated values of γ are used to estimate γM for use in successive iterations. The analysis was carried out using a digital computer and the iteration procedure was terminated when η changed by less than one part in 10^4 on successive iterations.

A common parameter used to describe microwave loss is the half-power linewidth ΔH . It is highly desirable to describe the field dependence of the relaxation rate in units which are compatible with the established convention. The discussion to follow is in terms of an effective linewidth ΔH_{eff} which is proportional to η and is related to ΔH . The meaning of ΔH_{eff} can be understood by considering a simplified susceptibility expression of the form

$$4\pi\chi_e''(L) = \frac{1}{2}\gamma 4\pi M \eta / [(\gamma H_0 - \omega)^2 + \eta^2]. \quad (3)$$

Equation (3) characterizes the usual absorption curve for ferromagnetic resonance obtained with a circularly polarized microwave field rotating in a Larmor sense. If η and γ are independent of H_0 , then Eq. (3) describes a Lorentzian curve centered at $H_0 = \omega/\gamma$ and with a linewidth given by $\Delta H = 2\eta/\gamma$. Absorption curves which are not Lorentzian can be described by Eq. (3) if η

and γ are allowed to be field-dependent and an effective linewidth can be defined by

$$\Delta H_{\text{eff}} = 2\eta(H_0)/\gamma(H_0). \quad (4)$$

The field dependences of η , γ , and ΔH_{eff} provide a measure of the departure of the absorption curve from a Lorentzian line shape. The effective linewidth magnitude and field dependence are determined primarily by $\eta(H_0)$. The gyromagnetic ratio γ does not change appreciably with H_0 and does not significantly alter the field dependence of ΔH_{eff} from that of η . For the present purposes, it is simply a normalizing parameter used to express η in linewidth units. The small changes in γ with H_0 are related to an effective line shift discussed previously by Motizuki *et al.*⁶ and Vrehan.⁹ Line shift is not considered here.

III. RESULTS

In Fig. 1 the field dependence of the effective linewidth ΔH_{eff} is shown for the series of porous YIG materials for values of the external field between 2500 and 4800 Oe. The data show that ΔH_{eff} is large in the field range 3000–4000 Oe and decreases outside this region. The effective linewidth also increases with porosity. The peak in ΔH_{eff} generally occurs at fields higher than that required for ferromagnetic resonance. The field for resonance at 9.96 GHz is indicated by the arrow at 3540 Oe. Furthermore, the curves exhibit considerable structure for the dense materials, as indicated by the double-peak behavior for YIG99 and the low-field shoulder for the YIG97. With decreasing density the curves broaden considerably and become more symmetric. These results are in contrast with Liu's data on normally magnetized YIG disks.⁷ He reported a

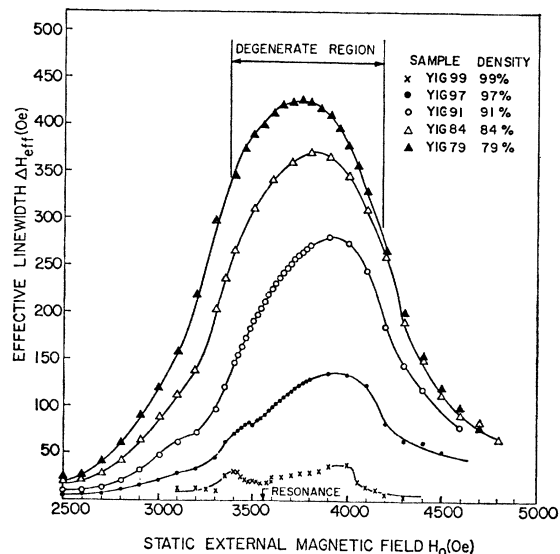


Fig. 1. Effective linewidth as a function of static external field for the series of porous polycrystalline YIG materials.

¹⁴ J. J. Green and T. Kohane, *Semicond. Prod.* **7**, No. 846 (1964).

¹⁵ T. L. Gilbert, *Phys. Rev.* **100**, 1243 (1955).

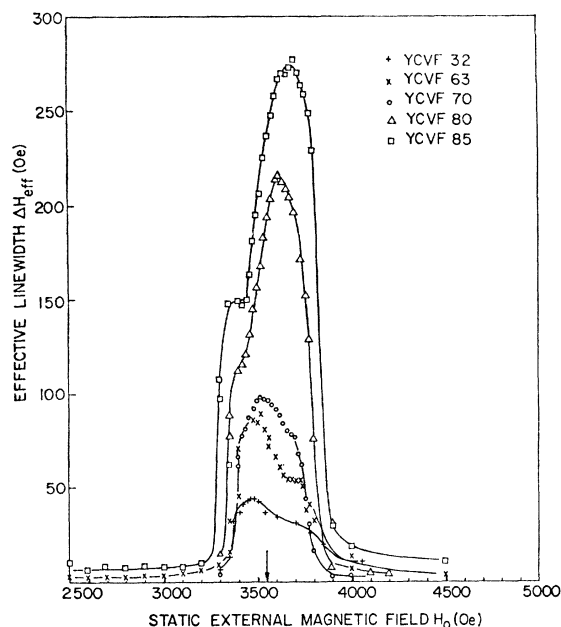


Fig. 2. Effective linewidth as a function of static external field for the series of YCVF materials.

relatively constant ΔH_{eff} for the field region corresponding to the peaks and structure in Fig. 1. His results were based on χ_e'' data only. Line-shift effects related to χ_e' are important in this field region^{6,9} and must be taken into account. These curves of effective linewidth versus applied static field are not to be confused with the conventional resonance absorption curves of χ_e'' versus H_0 . The vertical axis represents a *derived* quantity ΔH_{eff} which is related to the uniform-precession relaxation rate and is obtained from susceptibility data and the analysis procedure described in Sec. II. The conclusions concerning the effective linewidth and relaxation for porosity broadening pointed out above are not usually evident directly from the absorption curve. The analysis of data in terms of an equivalent relaxation rate or effective linewidth constitutes an extremely powerful technique for extracting quantitative information concerning the relaxation.

In Fig. 2 the corresponding results are shown for anisotropy broadening in the series of dense YCVF materials summarized in Table II. These materials were better than 99% dense, and porosity cannot be an important consideration in the results for these materials. The effective linewidth is generally large in a field interval 3200–3900 Oe and decreases sharply to a low and relatively constant value outside this interval. The effective linewidth inside this interval clearly increases with anisotropy field. In contrast with the YIG results, the symmetry of the effective linewidth field dependence changes from sample to sample. The low-anisotropy materials, such as YCVF32, 63, and 70, exhibit a peak in ΔH_{eff} at static fields lower than required for resonance. The resonance position is indi-

cated by the arrow at 3540 Oe. The ΔH_{eff} for these materials also exhibits a significant high-field shoulder at about 3700 Oe. Curves for the high-anisotropy materials such as YCVF80 and 85, on the other hand, exhibit broad peaks in ΔH_{eff} above resonance and low-field shoulders between 3300 and 3400 Oe. Figure 2 actually presents an oversimplified picture of the effective linewidth in the YCVF materials, particularly for the low-anisotropy YCVF32, 63, and 70 samples. If the contribution of anisotropy broadening to the relaxation is not large, it is reasonable to expect that various other inhomogeneity factors will influence the experimental results. Although the specific nature of these inhomogeneities has not been investigated, it has been found that their contribution of ΔH_{eff} could be minimized if the susceptibility data were obtained on annealed samples. Large spheres or unannealed materials exhibited large broad peaks in ΔH_{eff} at fields above resonance, which may be associated with a strain-induced inhomogeneity broadening. Annealing at 1000°C for 1 h was sufficient to eliminate the extraneous behavior. It is believed that the results in Fig. 2 provide an accurate description of the anisotropy contribution to ΔH_{eff} in the absence of such effects.

IV. THEORETICAL CONSIDERATIONS

Two processes that are expected to contribute significantly to the relaxation rate and ΔH_{eff} in polycrystalline YIG and YCVF materials are (a) two-magnon scattering processes related to local variations in the saturation induction caused by porosity or other magnetic inhomogeneities, and (b) two-magnon scattering related to local variations in the crystalline anisotropy from crystallite to crystallite. Two-magnon relaxation has been reviewed in detail by Sparks.¹ The purpose of this section is to emphasize several qualitative aspects of the process which are relevant to the present data, and to briefly describe two calculations by Motizuki *et al.*⁶ and Schlömann,¹⁶ respectively, which have been used to compute theoretical curves for comparison with the data in Figs. 1 and 2.

Two-magnon scattering is a mechanism by which the uniform-precession mode at the driving frequency loses energy through coupling to degenerate spin-wave modes. The coupling depends on the presence of inhomogeneities in the sample. In course-grained polycrystalline garnets such as YIG, with grain sizes on the order of microns, strong coupling can occur only to relatively long-wavelength modes with wave number k less than an inverse grain size. Such states are degenerate with the driving frequency only over a limited range of static magnetic field given by

$$H_{11} = \omega/\gamma + \frac{4}{3}\pi M > H_0 > [(2\pi M)^2 + (\omega/\gamma)^2]^{1/2} - \frac{2}{3}\pi M = H_1 \quad (5)$$

for spherical samples. In Eq. (5), H_{11} and H_1 are the

¹⁶ E. Schlömann, J. Appl. Phys. **40**, 1422 (1969).

external fields at which the degenerate low- k spin waves have \mathbf{k} parallel and perpendicular to H_0 , respectively. At intermediate fields the wave vector \mathbf{k} is at some angle $\theta_k (0 < \theta_k < \frac{1}{2}\pi)$ to H_0 . Outside the interval of Eq. (5), the scattering contribution to the relaxation rate (or ΔH_{eff}) is expected to be small. It would be zero except for the fact that the spin-wave levels are broadened because of the nonzero relaxation rate η_k for the states. Consequently, some coupling is expected even when the uniform mode is driven outside the degenerate region.

Qualitatively, ΔH_{eff} is expected to go through a maximum in the field interval of Eq. (5), and drop off to some smaller value outside that interval. The symmetry of this peak is related to the field dependence of the density of states degenerate with ω and the nature of the inhomogeneity which gives rise to the coupling. This density of states is quite large near $\theta_k = \frac{1}{2}\pi$ or $H_0 = H_{\perp}$ and vanishes at $\theta_k = 0$ or $H_0 = H_{\parallel}$. If the coupling strength is independent of θ_k , then ΔH_{eff} should peak near the low-field limit of Eq. (5) and be small near the high-field limit. This situation is expected for scattering due to crystalline anisotropy in randomly oriented crystallites.¹⁷ For scattering due to pores, the demagnetizing fields around pores are the source of the coupling. In this case, the coupling strength is a strong function of θ_k and is largest at $\theta_k = 0$, so that ΔH_{eff} due to porosity should peak near the high-field limit of Eq. (5).

The preceding discussion briefly outlines the basic features of two-magnon scattering relaxation in polycrystals. A number of early calculations describe these features in a more quantitative manner.¹⁸⁻²¹ The details of these calculations have been reviewed by Sparks.¹ For the most part, these calculations consider only interactions between the uniform mode and degenerate low- k modes. They do not take the relaxation of these modes into account. Consequently, they predict a zero η for $H_0 < H_{\perp}$ or $H_0 > H_{\parallel}$. The experimental results of Liu,⁷ of Kohane and Schlömann,⁸ and of Vrehan,⁹ as well as the present data, all indicate that ΔH_{eff} can be quite large outside this interval. Motizuki *et al.*⁶ and Schlömann¹⁶ have discussed the shortcomings of two-magnon calculations which do not take the spin-wave relaxation into account. They suggest that the large relaxation rates which occur when the uniform mode is driven outside the degenerate region may be due to spin-wave relaxation. Motizuki *et al.* consider scattering due to pores and include a

nonzero relaxation rate η_k for the low- k spin-wave modes in the calculation as an adjustable parameter. Their result is essentially an extension of the original Sparks pit-scattering theory to include spin-wave relaxation. The calculation results in a field-dependent effective linewidth which is similar to the data in Fig. 1. A comparison of the present porosity data with theoretical curves will be made in Sec. V. Schlömann has taken the spin-wave relaxation rate into account in a self-consistent manner by considering secondary two-magnon scattering between the degenerate low- k spin-wave modes. He considered the specific case of scattering due to crystalline anisotropy in the polycrystal. This case is somewhat easier to handle than that for porosity because the coupling is independent of θ_k . If relaxation other than two-magnon scattering is neglected, his results for ΔH_{eff} contain no adjustable parameters. The effective linewidth is completely specified in terms of $4\pi M$, H_A , H_0 , ω , and the sample demagnetizing factors. Schlömann's theory also indicates that the η_k which should be used in a phenomenological approach, such as presented in Ref. 6, is on the order of η . This value is much larger than the usual spin-wave relaxation rate inferred from parallel pumping. A comparison of the present data for the Ca-V garnets with curves obtained from Schlömann's theory is made in Sec. V.

V. COMPARISON WITH THEORY

The general features of the data for both the porous YIG materials (Fig. 1) and the vanadate garnets (Fig. 2) agree with the qualitative behavior of ΔH_{eff} expected for two-magnon scattering. The field intervals for large ΔH_{eff} values are somewhat larger than the interval of Eq. (5) for which low- k modes are degenerate with ω . This degenerate region is indicated in Fig. 1 for the YIG. The relatively large ΔH_{eff} outside this interval is due to the spin-wave relaxation or secondary scattering. The symmetries of the experimental curves agree with the qualitative considerations of Sec. IV. The purpose of this section is to provide a more quantitative comparison of the data with theory.

Consider the results for porous YIG. If the spin-wave relaxation rate η_k in the Motizuki *et al.* theory⁶ is assumed to be equal to the uniform-precession relaxation rate η evaluated at resonance, the theoretical curves in Fig. 6 of Ref. 6 for $2\eta_a/\omega_m = 0.01$ and 0.25 correspond quite closely to theoretical curves for YIG99 and YIG79, respectively.²² These two curves have been converted to plots of ΔH_{eff} versus H_0 for direct comparison with the data, as shown in Figs. 3 and 4. The theoretical curve in Fig. 3 for YIG99 was obtained assuming a porosity of 0.5%.

As shown by Fig. 3, the agreement for YIG99 is quite good. The position of the low-field peak, the

¹⁷ The scattering approach is valid only for relatively low anisotropy materials with $H_A \ll 4\pi M$. For high-anisotropy materials, the crystallites tend to resonate independently and the absorption curve is strongly influenced by crystallographic considerations. See E. Schlömann, *J. Phys. Chem. Solids* **6**, 257 (1958).

¹⁸ S. Geschwind and A. M. Clogston, *Phys. Rev.* **108**, 49 (1957).

¹⁹ M. Sparks, R. Loudon, and C. Kittel, *Phys. Rev.* **122**, 791 (1961).

²⁰ P. E. Seiden and M. Sparks, *Phys. Rev.* **137**, A1278 (1965).

²¹ E. Schlömann, *J. Phys. Chem. Solids* **6**, 242 (1958).

²² The abscissa δ in Fig. 6 of Ref. 6 corresponds to $u^2 - 1$, not to $1 - u^2$, where $u = \cos\theta_0$.

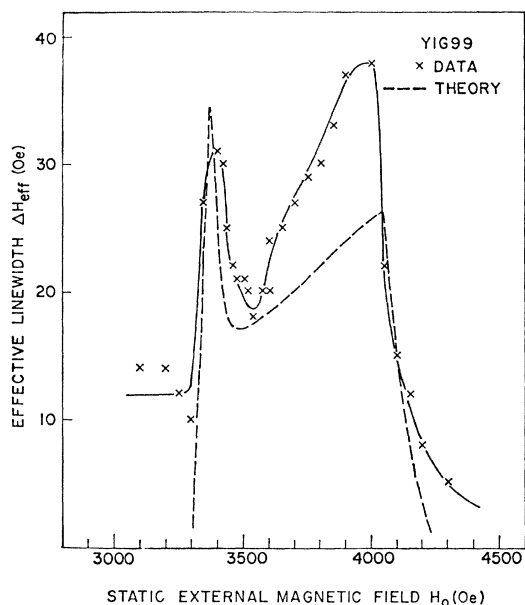


FIG. 3. Experimental data and theory for the effective linewidth as a function of static field for YIG99, the YIG with >99% theoretical density.

minimum near resonance, and the sharp reduction in ΔH_{eff} above 4050 Oe are accurately predicted by the theory. The shape of the theoretical curve for YIG79 in Fig. 4 agrees qualitatively with the experimental result even though the theoretical peak is much higher than observed experimentally and the theoretical curve falls off more steeply below resonance than the data. These results show that the Motizuki *et al.* theory can qualitatively explain the important features of the

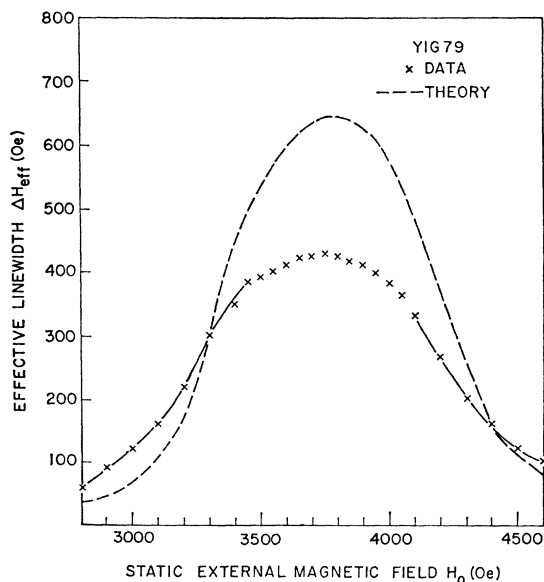


FIG. 4. Experimental data and theory for the effective linewidth as a function of static field for YIG79, the YIG with 79% theoretical density.

porous YIG data. The poor quantitative agreement is probably due to the lack of accurate estimates of η_k to use in the theory. The assumption $\eta_k = \eta$ (resonance) is not completely justified. Schlömann's result indicates that $\eta_k = \frac{1}{2}\eta$ is approximately correct, so that the η_k should vary with static field. The manner in which such refinements would affect the agreement has not been investigated. The agreement between the data and theory near resonance (3540 Oe) for YIG99 in Fig. 3 is somewhat misleading. Half of the observed ΔH_{eff} is probably due to anisotropy.¹² The theoretical minimum of 20 Oe is therefore much too high, since the Motizuki *et al.* theory did not consider anisotropy. This discrepancy may be due to the nonsphericity correction²⁰ applied to the original Sparks theory¹⁹ to account for the nonspherical shape of pits in real materials. (The theory assumes spherical pits.) This correction does not appear to be completely justified.²³ If it were removed, the theoretical minimum in ΔH_{eff} near resonance should be lowered significantly. All of these complications indicate that it is difficult to make any quantitative comparison of the data with the Motizuki *et al.* theory.

Now consider the results for the YCVF materials summarized in Fig. 2. Theoretical curves have been obtained from Schlömann's theory¹⁶ for comparison with the data. The curves were calculated by neglecting relaxation processes other than two-magnon scattering. As shown by Figs. 5-7, the agreement is quite good for YCVF32, 63, and 70, which all have anisotropy fields much less than $4\pi M$. From Fig. 5 the ΔH_{eff} for YCVF32 is slightly higher than expected theoretically. Residual inhomogeneities other than the anisotropy in randomly oriented crystallites are the most probable cause of this discrepancy. The agreement in Fig. 6 for YCVF63 is excellent. For YCVF70 the shape of the theoretical curve in Fig. 7 compares favorably with the data, although the magnitudes of the predicted effective linewidths are slightly larger than the experimental values. The results in Figs. 5-7 show that both the magnitude and symmetry of the ΔH_{eff} peaks can be accurately predicted from Schlömann's theory.

The theory, however, is not completely applicable to the higher-anisotropy YCVF80 and 85 materials with H_A on the order of $4\pi M$. It does predict the magnitude of the peak in ΔH_{eff} for YCVF80 and 85, but does not explain the symmetry of the data. In these materials the crystallites tend to resonate independently. Secondary peaks or shoulders appear in the absorption curve both above and below the main peak, which are related to the distribution of crystallite easy axes in the polycrystal. Such modifications of the absorption spectra are not taken into account in the procedure used to evaluate ΔH_{eff} from χ_e and also are not considered in Schlömann's theory.

²³ E. Schlömann, Raytheon Technical Memo No. T-747, 1967 (unpublished).

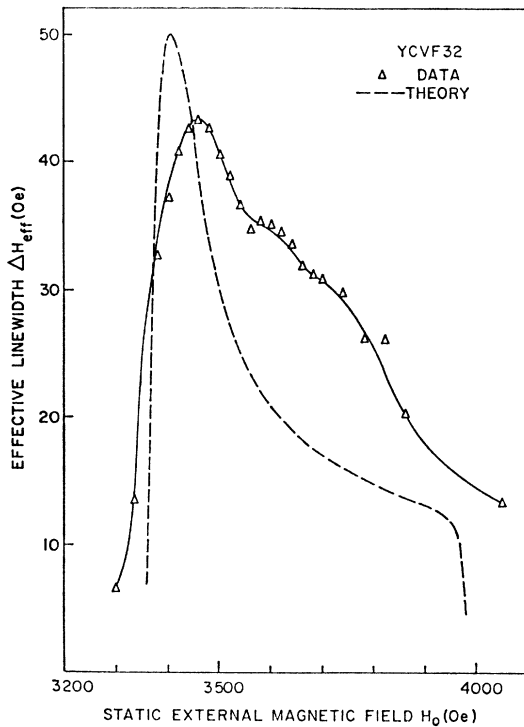


FIG. 5. Experimental data and theory for the effective linewidth as a function of static field for YCVF32, the YCVF material $Y_{3-2x}Ca_{2x}Fe_{5-x}V_xO_{12}$ with $x=0.32$.

VI. SUMMARY AND CONCLUSION

The purpose of this investigation was to examine the field dependence of the uniform-precession relaxation

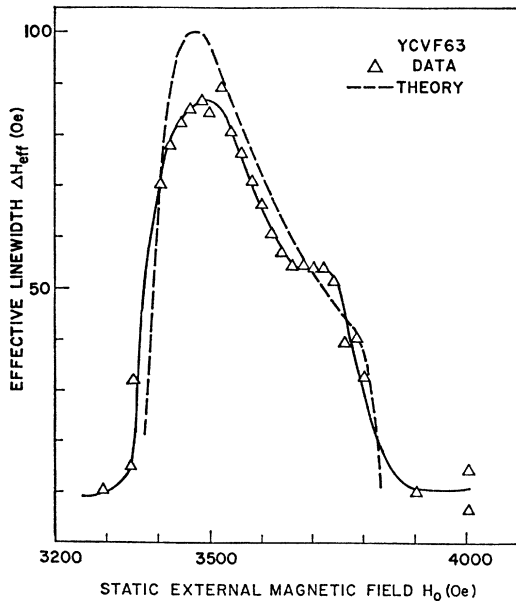


FIG. 6. Experimental data and theory for the effective linewidth as a function of static field for YCVF63, the YCVF material $Y_{3-2x}Ca_{2x}Fe_{5-x}V_xO_{12}$ with $x=0.63$.

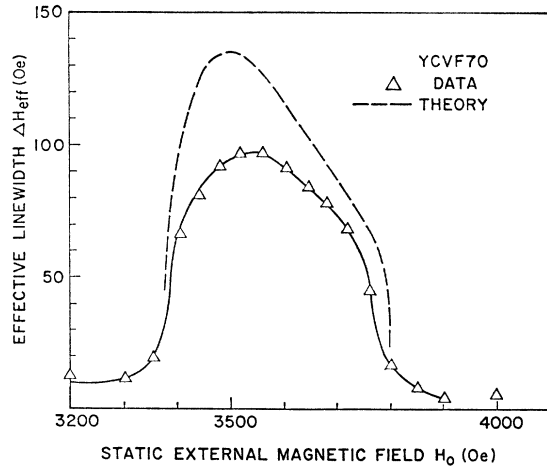


FIG. 7. Experimental data and theory for the effective linewidth as a function of static field for YCVF70, the YCVF material $Y_{3-2x}Ca_{2x}Fe_{5-x}V_xO_{12}$ with $x=0.70$.

rate in polycrystalline YIG as a function of porosity and in YCVF as a function of anisotropy, and to relate the experimental results to theoretical considerations of the two-magnon scattering contribution to the relaxation rate in polycrystals. The effective linewidth in polycrystals is significantly larger inside a field interval for which scattering to degenerate spin-wave states is allowed than for fields outside this interval. The effective linewidth exhibits a maximum in this field region, although the details of the ΔH_{eff} field dependence are a complicated function of porosity and anisotropy. Annealing history and sample size also influence the results. A large porosity results in a peak in ΔH_{eff} near the high-field side of the above field interval. Anisotropy results in a peak near the low-field side. A large contribution from either type of inhomogeneity, porosity or anisotropy, results in a broad maximum near the center of the interval. These results are consistent with theoretical predictions concerning the two-magnon scattering contribution to the relaxation rate if the relaxation of the low- k modes is taken into account.

ACKNOWLEDGMENTS

The author gratefully acknowledges E. Schlömann for many helpful discussions concerning relaxation theory, H. J. Van Hook for providing the YCVF materials and furnishing anisotropy data on these materials, and E. Q. Maguire for providing the YIG materials. He is also indebted to T. Kohane, who originally developed much of the instrumentation used in this study, and to H. J. Van Hook and J. Sage for editorial assistance. The author is extremely grateful to Miss S. Georgian for her careful and diligent attention to the microwave measurements.